Enhancing DC Microgrid Electrothermal Performance Through Digital Twin Enabled Droop Optimization

Cameron Ball, Kerry Sado, Emerson Miller, Emad Sadeghi, Jarrett Peskar, Connor Madden, Austin R.J. Downey, Adel Nasiri, and Enrico Santi

Department of Electrical and Computer Engineering
University of South Carolina, USA

This is a digest intended for submission to

IEEE APEC 2026 – IEEE Applied Power Electronics Conference and Exposition

[1]This work was supported by the Office of Naval Research under contracts No.N00014- 23-C-1012, and No.N00014-24-C-1301.

Enhancing DC Microgrid Electrothermal Performance Through Digital Twin Enabled Droop Optimization

Abstract– An optimized droop control strategy for a DC microgrid system integrating a fast-responding energy storage source and a slower generator source is presented. The objective is to optimize the droop gains to achieve optimal power sharing and voltage regulation while adhering to critical operational constraints including battery state of charge (SoC) limits, internal temperature management to prevent thermal runaway, and generator ramp rate limitations. A comprehensive optimization framework is developed, leveraging a digital twin for real-time estimations and initial system status. The work details the required MATLAB models for simulation and provides experimental validation, demonstrating the potential for enhanced microgrid performance, reliability, and sustainability through intelligent control. Full details will be provided in the full paper.

I. Introduction

DC microgrids are increasing in popularity due to their high efficiency, scalability, and suitability for integrating renewable energy sources and energy storage systems (ESSs). Their simplified control architectures and reduced conversion stages make them particularly suitable for naval platforms, remote off-grid installations, and mission-critical infrastructures [1], [2]. A key control challenge in DC microgrids involves managing power sharing among distributed sources, especially when integrating fast energy storage units, such as batteries, with slower mechanical generators. Droop control remains the most widely used method for power management because of its decentralized structure and ease of integration. Conventional resistive droop control schemes are effective during steady-state operation but typically result in significant voltage deviations and slower transient responses when subjected to rapid load changes [3]. The incorporation of a capacitive element into traditional droop schemes, forming RC droop control, has been demonstrated to enhance dynamic performance. This capacitive element introduces a derivative action, allowing the droop controller to respond quickly to voltage variations, thereby improving transient performance and overall system stability [4].

Many studies on droop control in hybrid source DC microgrids address proportional power sharing or transient performance using fixed gains [5], [6]. However, they often overlook critical system level constraints related to electrothermal limits of batteries and mechanical limitations of generators. Ignoring battery state-of-charge (SoC) constraints may cause excessive stress when

This work was supported by the Office of Naval Research under contracts No.N00014- 23-C-1012, and No.N00014-24-C-1301.

batteries are required to handle rapid load changes at low charge states, accelerating degradation, shortening cycle life, and risking thermal runaway [7]. Similarly, neglecting internal battery temperature and cooling system limitations can lead to overheating and subsequent shutdown or damage. Moreover, mechanical constraints, such as generator ramp rate limits, must also be considered to avoid mechanical fatigue and voltage instability during rapid load variations. Recent approaches employing adaptive methods, such as sliding mode control or rule-based supervisory control, have aimed at improving coordination between hybrid energy sources. However, these methods predominantly focus on electrical system performance, often disregarding critical constraints related to thermal and mechanical domain [8], [9].

This work proposes an optimization framework for RC droop control explicitly incorporating electrothermal constraints of battery systems and ramp-rate limitations of generators. Leveraging a digital twin architecture, the framework provides real-time state estimation and adaptive tuning of droop gains, ensuring safe and reliable operation under dynamic loading conditions.

II. System Description

The system under study, illustrated in Fig. 1, consists of a DC bus interconnecting two power converters and a variable load. The sources that the converters connect to are representative of an ESS and synchronous generator (SG), which impose power sharing constraints due to their physical characteristics. To address this, different droop schemes are applied to the two sources. For the ESS converter, capacitive droop control is employed to leverage the battery's ability to support fast-changing loads, characterized by the capacitive current relationship $I_{\mathrm{C}} = C\,\frac{dV}{dt}$. Equation (1) gives the capacitive droop equation, where v_{ref} is the commanded voltage reference, V_{nom} is the nominal voltage setpoint, C_{d} is the capacitive droop coefficient, and i is the measured current

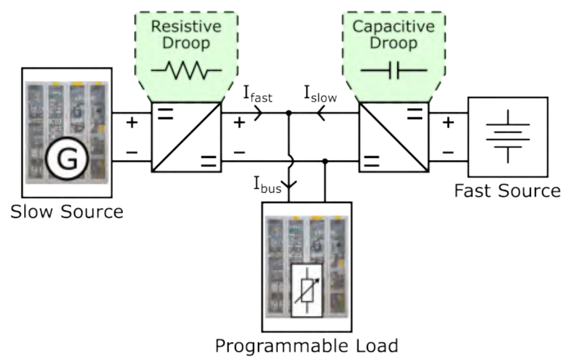

Figure 1: Schematic of the system under study.

$$v_{\mathrm{ref}}(t) = V_{\mathrm{nom}} - \frac{1}{C_{\mathrm{d}}}\int_0^t i(\tau)\,\mathrm{d}\tau. \tag{1}$$

For the converter on the generator side, resistive droop is employed because the ESS's capacitive droop inherently limits the power ramp rate of this slower dynamic source. The resistive droop equation is given by $v_{\mathrm{ref}}(t) = V_{\mathrm{nom}} - R_{\mathrm{d}}\,i(t)$, where the droop coefficient R_{d} scales the measured current, producing a voltage offset proportional to the load current.

III. Electro-thermal Battery Modeling and System Constraints

The electro-thermal battery model consists of a coupled sub-electrical and thermal model with interdependent responses. The sub-electrical model consists of a Coulomb counting approach in Equation (2) for estimating the SoC and a second order equivalent circuit model (ECM) representation of the battery

$$SoC(t) = SoC_0 + \frac{1}{C_{\text{bat}}} \int_0^t I(\tau)\, \mathrm{d}\tau. \tag{2}$$

The ECM, shown in Fig. 2, represents the battery as a voltage source, a single equivalent series resistance (R_{ohm}), and two series-connected parallel resistor-capacitor branches ($V_{R_1C_1}$ and $V_{R_2C_2}$). The voltage source is the open-circuit voltage (OCV) of the battery. The steady-state voltage drop and current through the battery are modeled using the equivalent series resistor R_{ohm}. The fast and slow transient voltage responses are enabled by two RC branches: the first with a fast time constant, and the second with a slow one.

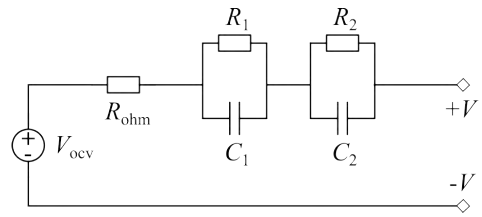

Figure 2: Battery second-order ECM representation.

The sub-thermal model is a lumped 1D heat transfer model. The battery pack is treated as lumped thermal mass (C_{pack}) with a heat generation term (Q_{gen}) and liquid cooling term (Q_{loss}). The lumped thermal mass is calculated as $C_{\text{pack}} = n_{\text{total cells}} \cdot m_{\text{cell}} \cdot c_{p,\text{cell}}$, where m_{cell} is the cell mass, $c_{p,\text{cell}}$ is the specific heat capacity, and $n_{\text{total cells}}$ is the total number of cells in the pack. The primary source of heat generated within the pack is joule heating, calculated by $Q_{\text{gen}} = n_{\text{total cells}} \cdot I^2(t) \cdot R_{\text{ohm}}(SoC, T)$. Because R_{ohm} is not constant over the SOC range of the battery, look-up tables are utilized to update R_{ohm}. For the heat loss, newtons law of cooling is applied between the pack and the liquid cooling system is represented by $Q_{\text{loss}} = -U \cdot A_{\text{conv}} \cdot LMTD$. With A_{conv} being the convective area, U, representing the multi-layer conduction from the pack to a cooling plate and convection to the water, and $LMTD$, the log mean temperature difference, driving the heat transfer.

IV. Optimization Framework and Experimental Results

An optimization framework was developed in order to achieve desired values for the battery state of charge, thermal values, and generator ramp rate. This framework outlined in Fig. 3 utilizes a model based optimization approach incorporating Simulink models to generate parameters for the objective function and constraints. The control variables are the resistive and capacitive droop parameters for the generator and battery respectively, R_{droop} and C_{droop}, that simultaneously minimizes internal temperature T_{in} and generator ramp-rate R_{ramp}, and maximizes battery SoC.

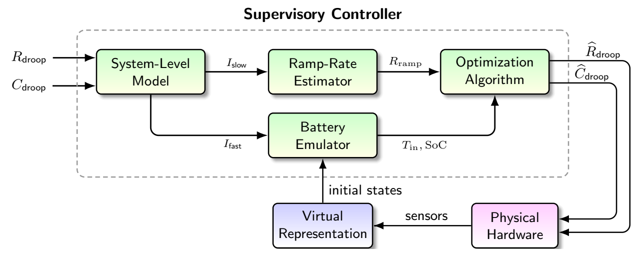

Figure 3: Digital-twin-enabled model-based optimization framework for droop control. The virtual representation simulates electro-thermal and ramp rate behavior in real time using system measurements, enabling adaptive tuning of droop gains through a supervisory controller.

The currents of the two sources, I_{fast} and I_{slow}, are passed to a battery emulator $\mathcal{E}_{\text{bat}}$ and a ramp-rate estimator $\mathcal{R}$, yielding $(T_{\text{in}}, SoC) = \mathcal{E}_{\text{bat}}(I_{\text{fast}})$ and $R_{\text{ramp}} = \mathcal{R}(I_{\text{slow}})$. Each quantity is therefore a deterministic function of $(R_{\text{droop}}, C_{\text{droop}})$. The objective function seeks to minimize the battery internal temperature T_{in}, and the ramp rate of the generator R_{ramp}, and maximize the battery SoC, as well as minimize the regularized droop parameters. The overall weighted objective function is:

$$J(R_{\text{droop}}, C_{\text{droop}}) = w_T\, T_{\text{in}} + w_R\, R_{\text{ramp}} - w_S\, SoC + \lambda_1 \left(\frac{R_{\text{droop}}}{R_{\text{max}}}\right)^2 + \lambda_2 \left(\frac{C_{\text{droop}}}{C_{\text{max}}}\right)^2, \tag{3}$$

with weights w_T, w_R, w_S and tunable regularization parameters λ_1 and λ_2 reflecting design priorities. The optimized gains are:

$$(\widehat{R}_{\text{droop}}, \widehat{C}_{\text{droop}}) = \underset{R_{\text{droop}}, C_{\text{droop}}}{\arg\min}\; J(R_{\text{droop}}, C_{\text{droop}}). \tag{4}$$

Operational limits (e.g., $T_{\text{in}} \le 0.9\,T_{\text{max}}$, $R_{\text{ramp}} \le 5kW$, and $0.2 \le SoC \le 0.8$) can be enforced as hard feasibility constraints or absorbed into the cost with large penalty terms. Penalties simplify the search by enabling rejection of infeasible candidates during generation and penalizing those that violate constraints throughout the optimization.

To examine the search space under these constraints, a genetic algorithm is employed. It initializes a random population of solution candidates, encoding the optimization variables $(R_{\text{droop}}, C_{\text{droop}})$. The Simulink model is used to compute the objective function scores for each member of the population. Based on these evaluations, crossover and mutation operations are performed to generate improved candidates after each iteration. The population is then evolved until convergence. Multiple optimization methods are planned to be implemented and compared, along with multiple load profiles analyzed in the full paper.

Table I. System parameters before and after optimization.

Parameter	Simulated Unoptimized	Simulated Optimized	Experimental Unoptimized	Experimental Optimized
R_{droop} , C_{droop}	1 , 0.5	0.549 , 2.171	1 , 0.5	0.549 , 2.171
R_{ramp} [kW/s]	7.13	3.34	7.09	3.48
ΔT_{in} [°C]	0.34	0.60	0.33	0.47
ΔSoC_{min} [%]	0.60	1.24	0.57	0.70
ΔV_{bus} [V]	17.87	8.01	21.52	8.10
$Q[W]$	2.12	3.78	2.59	3.85

[1]Highlighted values are those that are undesirable.

Hardware results were obtained through a power hardware in-the-loop system detailed in Fig. 1. The initial values of the parameters were set to be 50% SoC, 20°C for T_{in}, and V_{bus} at 400 V.

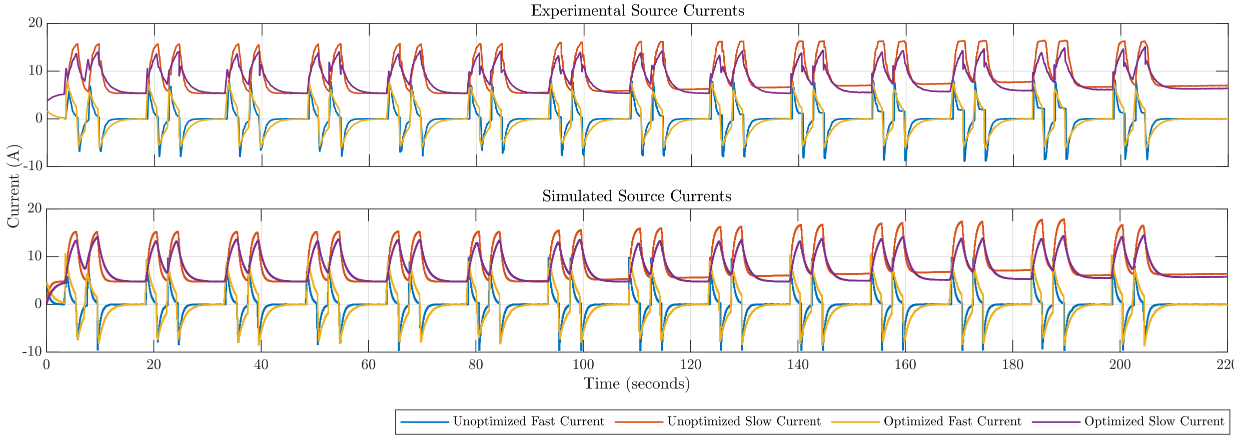

Figure 4: Experimental and simulated source currents for the unoptimized and optimized droop coefficients.

Comparison of experimental and simulated optimized and unoptimized source currents can be found in Fig. 4 and system parameters in Table I. In both unoptimized cases, the slow source has a ramp rate that exceeds the maximum value of 5 kW/s, and the fast source is under-utilized with ΔT_{in}, ΔSoC_{min}, and Q at low values. In the optimized cases, the ramp rate is decreased below 5 kW/s, and the battery is more fully utilized with higher ΔT_{in}, ΔSoC_{min}, and Q values. The increased thermal values are within acceptable bounds as to not accumulate excess heat in the simulated time frame of 220 seconds. Currently only the R_{ramp} value is deemed undesirable in the unoptimized cases; however, the full paper will provide analysis of additional load profiles and time frames.

V. Conclusions & Future Work

This work presented a droop control optimization strategy for DC microgrids that integrates a digital twin with electro-thermal modeling and ramp rate-aware control logic. The proposed method enables improved coordination between a fast dynamic source such as a battery and a slow dynamic source such as a generator, while maintaining key system constraints, including battery SoC, internal temperature, and generator ramp rate. The digital twin provides real-time system estimation and supports adaptive tuning of droop parameters based on system conditions. Simulation and experimental results verify the effectiveness of the optimization framework in reducing generator ramp rates, improving battery utilization, and maintaining thermal safety. The optimized control reduces mechanical stress on the generator by ensuring ramp rate compliance, which is expected to minimize wear and tear and extend generator lifespan over long-term operation. These improvements were achieved while satisfying all operational limits under representative dynamic load profiles. The full paper will include additional scenarios with varied load conditions and comparisons of optimization tools such as particle swarm and gradient-based methods. Future work will extend the framework to multi-source systems with predictive scheduling.

REFERENCES

[1] S. Anand and B. G. Fernandes, "Optimal voltage level for dc microgrids," in *IECON 2010 - 36th Annual Conference on IEEE Industrial Electronics Society*, 2010, pp. 3034–3039.

[2] J. M. Guerrero, M. Chandorkar, T.-L. Lee, and P. C. Loh, "Advanced control architectures for intelligent microgrids—part i: Decentralized and hierarchical control," *IEEE Transactions on Industrial Electronics*, vol. 60, no. 4, pp. 1254–1262, 2013.

[3] K. Yogithanjali Saimadhuri and M. Janaki, "Advanced control strategies for microgrids: A review of droop control and virtual impedance techniques," *Results in Engineering*, vol. 25, p. 103799, 2025. [Online]. Available: https://www.sciencedirect.com/science/article/pii/S2590123024020425

[4] Q. Xu, X. Hu, P. Wang, J. Xiao, P. Tu, C. Wen, and M. Y. Lee, "A decentralized dynamic power sharing strategy for hybrid energy storage system in autonomous dc microgrid," *IEEE Transactions on Industrial Electronics*, vol. 64, no. 7, pp. 5930–5941, 2017.

[5] S. A. Hamad, M. A. Ghalib, M. F. Elmorshedy *et al.*, "Optimizing power sharing accuracy in low voltage dc microgrids considering mismatched line resistances," *Scientific Reports*, vol. 14, p. 30195, 2024. [Online]. Available: https://doi.org/10.1038/s41598-024-74682-0

[6] H. Du, T. B. Hashfi, R. Prasad, P. P. Vergara, P. Palensky, and A. Lekić, "Optimal droop control strategy for coordinated voltage regulation and power sharing in hybrid ac-mtdc systems," 2025. [Online]. Available: https://arxiv.org/abs/2505.03651

[7] H. Yang, N. Zhang, and B. Gao, "The dc microgrid-based soc adaptive droop control algorithm," *Journal of Circuits, Systems and Computers*, vol. 32, no. 12, p. 2350205, 2023. [Online]. Available: https://doi.org/10.1142/S0218126623502055

[8] A. J. Abianeh and F. Ferdowsi, "Sliding mode control enabled hybrid energy storage system for islanded dc microgrids with pulsing loads," *Sustainable Cities and Society*, vol. 73, p. 103117, 2021. [Online]. Available: https://www.sciencedirect.com/science/article/pii/S2210670721003991

[9] M. A. Sharaf, H. Armghan, N. Ali, A. Yousef, Y. S. Abdalla, A. R. Boudabbous, H. Mehdi, and A. Armghan, "Hybrid control of the dc microgrid using deep neural networks and global terminal sliding mode control with the exponential reaching law," *Sensors*, vol. 23, no. 23, 2023. [Online]. Available: https://www.mdpi.com/1424-8220/23/23/9342